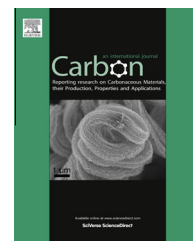


Available at www.sciencedirect.com

ScienceDirect

journal homepage: www.elsevier.com/locate/carbon

Promoter-assisted chemical vapor deposition of graphene

Ya-Ping Hsieh ^{a,*}, Mario Hofmann ^b, Jing Kong ^c

^a Graduate Institute of Opto-Mechatronics, National Chung Cheng University, 168 University Road, Minhsiung Township, Chiayi County 62102, Taiwan

^b Department of Materials Science and Engineering, National Cheng Kung University, No. 1, University Road, Tainan city 70101, Taiwan

^c Department of Electrical Engineering, Massachusetts Institute of Technology, 77 Massachusetts Avenue, Cambridge, MA 02139, USA

ARTICLE INFO

Article history:

Received 24 July 2013

Accepted 8 October 2013

Available online 16 October 2013

ABSTRACT

The synthesis of graphene by chemical vapor deposition (CVD) is a promising approach for producing graphene for novel applications. Especially graphene synthesis on Copper substrates has resulted in high quality, large area graphene growth. This method, however, exhibit limitations in achievable graphene quality due to the low catalytic activity of the growth substrate and occurring catalyst deactivation at high graphene coverage. We here study the effect of adding a material to promote graphene growth on Cu. Catalytic materials such as Nickel and Molybdenum were found to affect the graphene quality and growth rate positively. The origin for this enhancement is a decrease of the energy barrier of catalytic methane decomposition through a process of distributed catalysis. This process can also help overcome the issue of catalyst deactivation and increase film continuity. These findings not only provide a route for improving the CVD synthesis of graphene but also answer fundamental questions about graphene growth.

© 2013 Elsevier Ltd. All rights reserved.

1. Introduction

Graphene, a two-dimensional carbon allotrope, has recently received significant attention due to its unique physical properties and potential applications in a multitude of fields ranging from biology to material science and electronics [1]. To realize these promises large area graphene with high spatial uniformity and good crystalline quality has to be synthesized. Chemical vapor deposition (CVD) has proven to be a suitable synthesis method for such requirements [2] and especially the low pressure synthesis on Cu substrates can provide a robust method for the scalable production of single layer graphene [3]. Consequently, considerable research effort is being invested in optimizing the CVD process to improve the grain size and affect the crystallinity of graphene growth on Cu [4–6]. At the same time deeper understanding has been

gained through theoretical work to understand the limits of achievable graphene quality [7–9].

Two issues have been identified, both experimentally and theoretically, that limit the quality of graphene during CVD growth. First, the loss of catalytic activity of the growth substrate at high graphene coverage, a process known as “coking” in catalysis, is preventing the formation of continuous graphene [7] and openings between single crystalline grains remain and deteriorate graphene properties [10]. Second, the low catalytic activity of Cu substrate makes high temperature and long growth times necessary [8] which limits the throughput and commercial appeal of thus synthesized graphene.

We here present promoter-assisted CVD as a promising approach to overcome these issues. This approach is inspired by the traditional use of heated filaments in diamond CVD

* Corresponding author.

E-mail address: yphsieh@ccu.edu.tw (Y.-P. Hsieh).

0008-6223/\$ - see front matter © 2013 Elsevier Ltd. All rights reserved.

<http://dx.doi.org/10.1016/j.carbon.2013.10.013>

that result in higher quality material and a lowering of the required process temperature [11]. In our experiments a second catalytic material was introduced in the CVD process to assist the production of graphene on the Cu substrate. Improvements in graphene growth rate, total coverage, and graphene quality using this method were observed. The role of promoters on the growth kinetics was elucidated and a promoter-assisted lowering of the energy barrier of methane decomposition was found. Finally, the effect of promoters on catalyst deactivation and achievable graphene surface coverage was investigated.

2. Experimental

In our experiments, graphene was synthesized by CVD using copper as the catalyst material as previously reported [12]. Briefly, under low pressure (400 mTorr) a piece of copper foil (Alfa 13382) was used without any type of pretreatment and annealed in 20 sccm hydrogen at 1000 °C for 30 min. After annealing, 15 sccm methane gas was introduced to initiate the graphene growth. The formation rate of graphene was controlled by adjusting the flow rate of hydrogen. The pressure in the reaction chamber could be varied independently of the gas flow rates by closing a gate valve at the exhaust. After the synthesis was completed, the material was cooled down under 210 mTorr of hydrogen to prevent oxidation and minimize hydrogenation reactions of the graphene.

3. Results

In our experiments, graphene synthesized by traditional low-pressure CVD was compared to graphene produced by promoter-assisted CVD. Nickel was chosen as a first promoter since the methane decomposition on Nickel (111) surfaces

is expected to be more efficient than on copper [13,14]. This property in combination with the proven ability of Nickel to catalyze graphene growth makes it a promising candidate for a promoter [2].

We positioned a 10 × 20 mm piece of Nickel foil (Alfa Aesar 44822) upstream of the Cu-foil and conducted the CVD growth (see Fig. 1(a)). The graphene generated on the Cu-foil was then transferred onto Si/SiO₂ samples.

The quality of thus generated graphene was evaluated using Raman spectroscopy as detailed in the [Supplementary material](#). The graphene defectiveness can be quantified by analyzing the intensity ratio of the Raman D-Band and G-band features. The D-Band feature originates from a second order Raman scattering process involving an optical K-point phonon and a defect, while the G-band intensity I_G scales with the number of sp²-carbon bonds [15]. Consequently the I_D/I_G ratio reflects a measure of the relative defectiveness of graphene. Fig. 1b and c show the spatial variation of I_D/I_G for samples grown without and with a Ni promoter, respectively. The regions of high defectiveness seem to form loops and lines in agreement with previous observations that domain boundaries between incompletely merged graphene-grains have a larger defect signal [16].

Use of a promoter is found to decrease the intensity of those defects when comparing the Raman maps in Fig. 1b and c, which indicates that the continuity of graphene was increased. This finding was furthermore quantified by analyzing the number of Raman spectra within a certain interval of I_D/I_G . We observe that graphene grown with a Ni promoter on average exhibits a 30% lower I_D/I_G ratio with a smaller variation throughout the sample compared to samples grown on bare Cu.

The histogram in Fig. 1e furthermore reveals that the use of a promoter results in graphene with a red-shifted G'

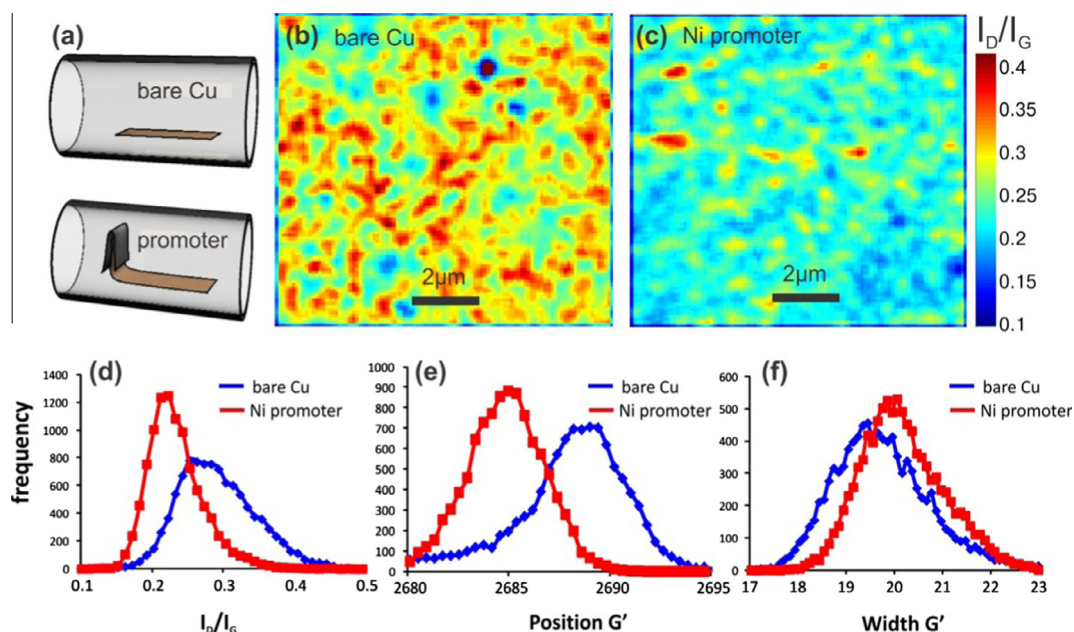


Fig. 1 – (a) schematic of Cu-substrate without and with promoter (b–c) Raman I_D/I_G map for graphene grown (a) without a promoter, (b) with a Ni promoter. (d–f) Histograms of Raman features without and with use of Ni promoter. (A color version of this figure can be viewed online.)

feature which can be attributed to a decrease in electrostatic doping [15]. This observation can be explained by a reduction in the density of dangling bonds for less defective graphene, which results in a decreased charge transfer between adsorbed oxygen molecules and the graphene [17]. Finally the width of the G' feature was analyzed in Fig. 1f and it was found that the use of a Ni promoter does not cause a significant broadening of the G' peak which indicates that the amount of bi-layer graphene regions was not increased [15]. These results demonstrate that the use of promoters creates graphene with less defects and lower doping while retaining control over the single-layer character of graphene.

We now attempt to explain the observation that the presence of Ni improves the graphene quality grown on a Cu substrate in its vicinity. To this end the spatial variation of the graphene coverage was analyzed with respect to the promoter.

The graphene surface coverage is commonly analyzed by scanning electron microscopy [6]. This method, however, fails at high surface coverage and is not able to identify small openings between merging grains [10] that are expected to be the origin of the observed I_D/I_G spatial variation in Fig. 1.

We have recently developed “film induced frustrated etching” (FIFE) as a metrology tool that is sensitive to openings of nanometer size in two dimensional films [18]. The technique was found to be useful to visualize the gaps between neighboring graphene domains and film imperfections at high graphene coverage. FIFE can be carried out directly on the growth substrate without the need for a transfer step. Briefly, a copper substrate covered with graphene is exposed for 10 s to Transene APS-100 copper etchant. Only copper regions that are not protected by graphene are attacked by the etchant.

Thus, the resulting change in Cu morphology after etching reveals information about the continuity of the graphene.

The beneficial effect of a promoter on the graphene coverage is illustrated when comparing two representative AFM images (Fig. 2a and b) taken at different distances from a Molybdenum promoter. It can be seen that close to the promoter there are fewer etch pits in the copper foil, indicating that the protecting graphene layer exhibits an increased continuity compared to graphene grown further away from the promoter. A similar behavior was also observed for the Ni promoter which supports that these materials increase the graphene coverage on Cu.

The relative unetched area (θ) after FIFE can be used to quantify this observation. The parameter θ can be extracted directly from the total hole area in an AFM image and is proportional to the graphene surface coverage as detailed in the [Supplementary information](#).

Fig. 2(c) confirms our previous observation that the graphene surface coverage is significantly improved by the presence of a promoter. The symmetric profile of $\theta(x)$ furthermore suggests that the coverage is not determined by flow or temperature effects, since these factors would result in a monotonic variation across the sample. Instead, we hypothesize that diffusion is the most important process in the interaction of the promoter with the growing graphene. Based on this observation, we suggest a simple process of distributed catalysis as the working principle of the promoter. First, carbon radicals are catalytically generated by the promoter and diffuse away from it. They are then incorporated into the graphene lattice on the growth substrate by a second catalytic process. Thus, the graphene growth process, which is normally accomplished by the growth substrate is divided

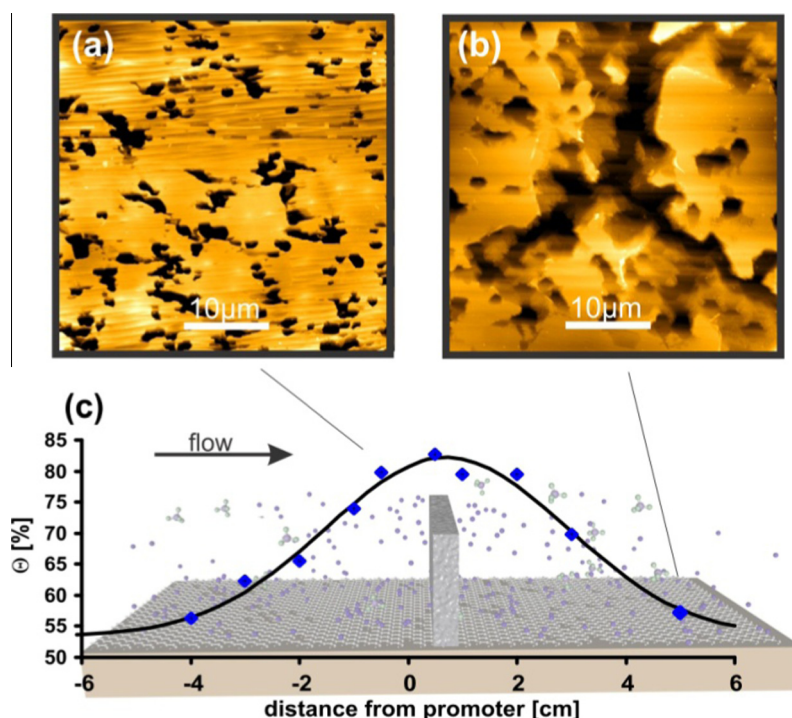


Fig. 2 – (a and b) representative AFM images taken at different distances, (c) θ vs. distance from Mo promoter (AFM image location indicated by the arrows). (A color version of this figure can be viewed online.)

between two elements in the case of promoter-assisted graphene growth.

The proposed model suggests that the graphene surface coverage is determined by the carbon radical concentration generated by either the promoter or the Cu substrate itself. Therefore, the spatial distribution $\theta(x)$ is expected to depend on factors influencing the carbon radical concentration, such as the diffusion coefficient of a given radical, its reaction rate to forming other carbon species, temperature induced variations of the diffusivity, convective mass transport due to the gas flow, etc. Realistic predictions that reflect these complex processes can be done by numerically solving the diffusion-reaction-equations using empirical parameters.

An analytical solution of the diffusion reaction equation for the presented experimental conditions can be attempted, since some of the described process parameters are expected to have only a small effect on the concentration profile and can be neglected: As shown in [Supplementary Fig. S3](#) the temperature variation over the sample is small and is not expected to be of significant influence. Also, for LPCVD growth the Sherwood number, which compares convective and diffusive mass transfer coefficients, is small [19]. Therefore, the convective transport (i.e. flow) is expected to be negligible compared to diffusive transport.

Thus, the main factors controlling the carbon radical density are diffusion and reaction processes, which are predicted to vary symmetrically around the promoter. These processes are expected to give rise to a concentration profile of the form:

$$C(x) = C_0 \exp\left(-x/\delta\right) + C_1 \quad (1)$$

where C_0 is the concentration of carbon species close to the promoter, x is the distance from the promoter, $\delta = \sqrt{D/r}$ is the ratio of the diffusivity of the carbon species D and its reactivity r and C_1 is a constant concentration caused by the

catalytic generation of the carbon species by the copper substrate.

The solid line in [Fig. 2c](#) represents a fitting of the experimental data of $\theta(x)$ to Eq. (1). From this fitting we obtain a value of $\delta = 1$ cm which is comparable to the length scales of the numerical solutions for the carbon radical decay at low pressure in the gas stream (see [Supplementary Information](#)). This agreement suggests that the main decay pathway for carbon radicals is their recombination in the gas stream and not carbon radical recombination on the Cu surface. Furthermore, the measured decay length is significantly larger than the length scales of metal inter-diffusion thus ruling out that the promoter is simply alloying with the Cu substrate [20]. The absence of alloying was also confirmed by X-ray photoelectron spectroscopy (see [Supplementary information](#)). The excellent agreement between the measured graphene coverage and the analytical solution of the diffusion-reaction equation shows that the graphene surface coverage is indeed determined by the radical concentration.

These experiments confirm the role of the promoter as a source of carbon radicals and support the distributed catalysis model. Subsequent experiments are aiming at understanding the origin of this effect.

The kinetics of the graphene growth were analyzed by studying the temperature dependence of the graphene growth rate. The coverage of graphene after 10 min growth was found to increase for higher growth temperatures as seen when comparing the morphology of graphene after FIFE testing ([Fig. 3a–c](#)). This observed proportionality between temperature and coverage ([Fig. 3d](#)) indicates a thermally activated growth process.

[Fig. 3\(e\)](#) shows an Arrhenius plot of the change in θ with temperature normalized to the value at 1000 °C. The activation energy of the rate limiting process step can be extracted from the slope in the Arrhenius plot according to Eq. (2).

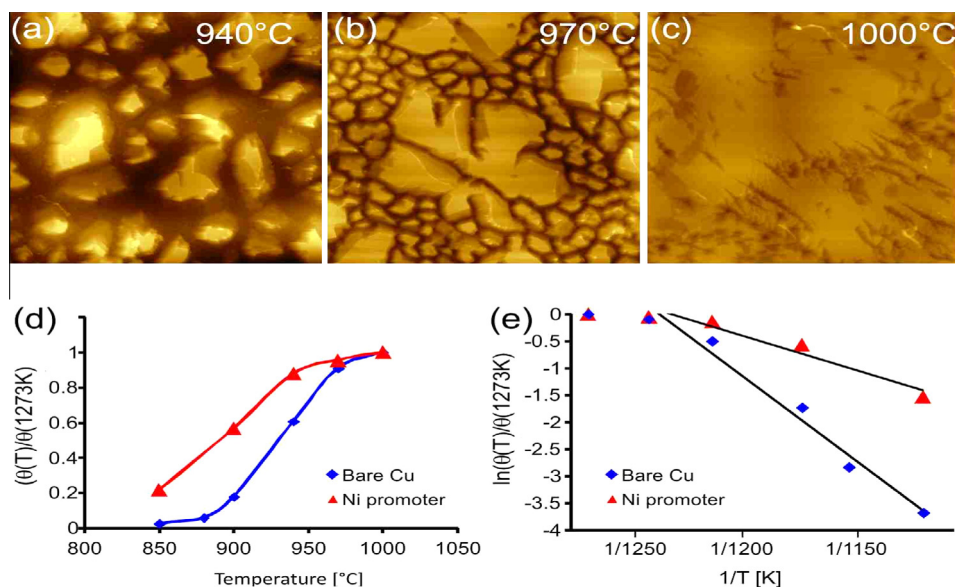


Fig. 3 – (a–c) AFM morphology of samples grown for 10 min at different temperatures after 10 s etch (d) θ normalized to value at 1000 °C as a function of temperature with and without Ni promoter (e) Arrhenius plot of same data (deviation from line at 1000 °C is due to merging of individual grains). (A color version of this figure can be viewed online.)

$$k_{2D} = Ae^{-E_a/2k_B T} \quad (2)$$

where A is a proportionality constant, T is the growth temperature in Kelvin and E_a is the activation energy barrier of the reaction step.

For bare Copper the activation energy was determined to be 3.7 eV while in the case of the Ni promoter a lower activation energy of 1.5 eV was found. These energy barriers are close to the theoretically predicted activation energies for the dehydrogenation reaction of methane to atomic carbon radicals on copper (3.6 eV [14]) and on nickel (1.32 eV [13]).

This agreement suggests that at the investigated growth condition the decomposition of methane into atomic carbon has a higher energy barrier than other reaction steps occurring during growth. The catalytic hydrogenation reaction proceeds more efficiently on Ni than on Cu-substrate and therefore Ni can produce carbon radicals which are subsequently incorporated into the graphene lattice on the Cu-substrate.

This observation has several important implications. First, the growth temperature of graphene can be decreased by using a promoter, since less thermal energy is required to form carbon radicals. Furthermore, the lowering of the rate limiting step will result in an increase in growth rate and consequently lower growth times. Finally, suitable promoters would not exhibit a decrease in catalytic activity as reported for Cu [7] at high graphene coverage.

The remainder of the paper will therefore investigate the effect of the promoter on the limits of achievable graphene coverage. This high coverage regime was analyzed for the first time due to the advantages of FIFE over traditional metrology tools in examining small openings between incompletely merged grains.

Previous reports reported the decrease in growth rate of graphene domains during the growth process brought about by the decreasing reactivity of the Cu substrate due to the deactivation of topochemical reaction sites at high graphene coverage. This phenomenon known in catalysis as “catalyst poisoning” or “coking” [21] results in incompletely grown graphene and deteriorates its performance [10]. The effect of catalyst poisoning is illustrated in the right inset of Fig. 4a. It is shown that graphene grown at low pressure is not continuous even after 90 min growth duration.

Based on the presented model of “distributed catalysis” the addition of a promoter is expected to increase the film quality since the promoter can supply carbon radicals without being covered and deactivated by graphene during the synthesis process. We indeed find that promoters can increase the continuity of the graphene. The use of a Mo-promoter, for example, results in a higher coverage after only 30 min growth than growth on bare Cu after 90 min as seen when comparing the insets of Fig. 4a.

To study the effect of different promoters on the growth of graphene, optimal growth conditions for each promoter were used. Since the efficiency of the catalytic decomposition of methane sensitively depends on the catalyst used, the methane partial pressure for each promoter had to be adjusted. For each promoter, $\theta(t)$ plots were rescaled by the methane exposure, which is calculated as the product of methane partial pressure and growth time. Fig. 4a shows the evolution of θ with methane exposure for Cu samples grown with and without the use of promoters.

When focusing on the high graphene coverage regions, it can be seen that the addition of either Mo and Ni promoters can increase the maximum θ to $\sim 90\%$. This value is thought to represent full graphene coverage at the used etching time and in the presence of surface impurities [18].

We also found that, when using molybdenum as a promoter, no graphene growth is observed on the Cu substrate during the initial 25 kPasec exposure. This induction period was previously observed for molybdenum promoters in methane reforming and attributed to the reaction of methane and molybdenum to form catalytically active molybdenum carbide [22] as detailed in the [Supplementary Information](#).

The time evolution of the surface coverage can reveal the activation energy at high coverage associated with the closing of the gaps between grains [9]. In the high surface coverage regime the growth rate not only depends on the reaction energy barriers but decreases through catalyst deactivation. This effect can be incorporated into a simple Langmuir model by assuming the reaction rate to scale with the availability of surface reaction sites.

Thus, the change of graphene coverage with time can be expressed as:

$$\frac{d\theta}{dt} = k_{2D}(1 - g\theta) \quad (3)$$

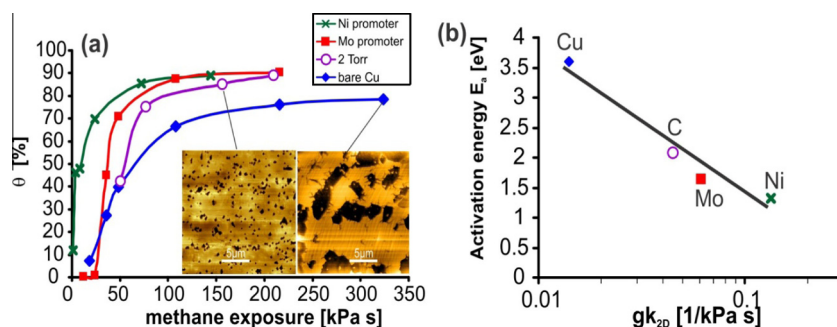


Fig. 4 – (a) θ vs. methane exposure for bare Copper, Molybdenum, Nickel promoters and higher pressure CVD growth, inset AFM morphology after 10 s etch, (right) 90 min growth on bare Cu, (left) 30 min growth with Mo promoter, (b) measured growth rate vs. theoretical activation energy barriers for methane dehydrogenation over different catalysts. (A color version of this figure can be viewed online.)

where k_{2D} is the growth rate of the graphene and the parameter g is introduced to express the importance of covered surface reaction sites to maintaining the growth process.

For low graphene surface coverage the number of covered sites is negligible and g tends to zero. In this case Eq. (3) converges to the previously used constant growth rate

$$k_{2D}(t) \approx \frac{\theta(t)}{\theta_{max}}$$

For the complete growth process the time evolution of the graphene surface coverage follows the function

$$\theta(t) = \theta_{max} \left(1 - e^{-gk_{2D}(t-t_0)} \right) \quad (4)$$

where t_0 is the previously described induction period, and k_{2D} is the growth rate at a certain methane pressure. The parameter θ_{max} includes the contribution of g and is thus depending on the process parameters.

In Fig. 4b the correlation between the extracted pseudo-growth rate gk_{2D} and the theoretically predicted activation energies for methane decomposition are plotted on a semi-logarithmic scale. It can be seen that they follow an Arrhenius-type behavior as expected from Eq. (1). We can therefore conclude that the promoter assisted lowering of the activation energy barrier of methane dehydrogenation not only affects the growth rate at low graphene coverage but also at high coverage. The combination of high growth rate and achievable full graphene coverage highlights the advantages of promoter assisted graphene CVD.

Interestingly, a high maximum coverage at large exposures is also achieved when reproducing a strategy used by Li et al. [4] that employs a higher pressure CVD step at 2 Torr. The extracted growth rate for this procedure agrees well with the predicted energy barrier for methane decomposition using activated carbon as a catalyst [23]. This observation can be explained by results obtained by Becker et al. [24], who found that an increase of methane partial pressure at high temperatures will result in an exponential increase in auto-catalytically generated carbon radicals. Thus, methane itself can act as the promoter and assist growth on the copper substrate. Based on this finding it can be inferred that graphene growth on copper is only self-limited at low methane pressure, when no autocatalytic production of carbon radicals occurs. At higher methane partial pressure, carbon radicals are being supplied even after complete graphene coverage is achieved. This behavior was confirmed for growth with promoters at very high methane exposure which results in the formation of amorphous carbon particles on the graphene film (Supplementary Fig. S7). This observation suggests that optimization of the carbon radical concentration could be a viable route to growing multiple graphene layers on Cu and could explain the production of bilayer graphene under growth conditions with higher methane pressure [12].

4. Conclusion

Based on the here presented analysis, requirements and limitations of promoters can be identified. First, a low activation energy for the methane decomposition is desirable for a high growth rate, and many additional promoters could be

selected based on this criterion, i.e. Ru ($E_a = 1.12$ eV), Pd ($E_a = 0.79$ eV) or Pt ($E_a = 1.2$ eV) [25].

There is a limit, however, to the achievable decrease of the activation energy barrier. If any other reaction step of the graphene growth exhibits a higher activation energy barrier it will become rate limiting. Theoretical predictions suggest that the graphene lattice formation on Cu substrates is 1.01 eV [26] which represents the second highest reaction step. This process is not expected to be affected by promoter-assisted CVD and limits the achievable graphene growth rate to a value approximately one order of magnitude higher than growth on bare Cu.

Finally, the mechanism of distributed catalysis allows to increase the list of potential growth substrates to materials that do not have the ability to decompose methane but facilitate the formation of the graphene structure such as metal oxides, dielectrics, carbides etc. [27–29].

In conclusion, we have investigated the effects of a promoter on the growth of graphene by CVD. Raman spectroscopy reveals a decrease of the graphene defectiveness and doping when adding a second catalytic material in the vicinity of a Cu growth substrate. The role of the promoter was found to be a reduction in the energy barrier of the methane dehydrogenation reaction. Through “distributed catalysis”, the promoter can efficiently perform the dehydrogenation reaction to provide carbon radicals that are incorporated into the graphene lattice by the Cu substrate. The use of Ni and Mo as promoters was found to overcome issues of catalyst deactivation and increase the achievable surface coverage. Due to the presented potential of sensitively controlling the carbon radical concentration and the ease of implementation, we recommend to consider the use of a promoter for future CVD growth of graphene.

Acknowledgements

Y. P. Hsieh acknowledges support under NSC-100-2112-M-194-006-MY3. M. Hofmann acknowledges support under NSC-101-2112-M-006-017-MY3 and D102-33B07. J. Kong acknowledge support under ONR MURI N00014-09-1-1063.

Appendix A. Supplementary data

Supplementary data associated with this article can be found, in the online version, at <http://dx.doi.org/10.1016/j.carbon.2013.10.013>.

REFERENCES

- [1] Geim AK. Graphene: status and prospects. *Science* 2009;324(5934):1530–4.
- [2] Reina A, Jia X, Ho J, Nezich D, Son H, Bulovic V, et al. Large area, few-layer graphene films on arbitrary substrates by chemical vapor deposition. *Nano Lett* 2009;9(1):30–5.
- [3] Li X, Cai W, An J, Kim S, Nah J, Yang D, et al. Large-area synthesis of high-quality and uniform graphene films on copper foils. *Science* 2009;324(5932):1312–4.

- [4] Li X, Magnuson CW, Venugopal A, An J, Suk JW, Han B, et al. Graphene films with large domain size by a two-step chemical vapor deposition process. *Nano Lett* 2010;10(11):4328–34.
- [5] Wood JD, Schmucker SW, Lyons AS, Pop E, Lyding JW. Effects of polycrystalline Cu substrate on graphene growth by chemical vapor deposition. *Nano Lett* 2011;11(11):4547–54.
- [6] Colombo L, Li X, Han B, Magnuson C, Cai W, Zhu Y, et al. Growth kinetics and defects of CVD graphene on Cu. *ECS Trans* 2010;28(5):109–14.
- [7] Kim H, Saiz E, Chhowalla M, Mattevi C. Modeling of the self-limited growth in catalytic chemical vapor deposition of graphene. *New J Phys* 2013;15(5):053012.
- [8] Kim H, Mattevi C, Calvo MR, Oberg JC, Artiglia L, Agnoli S, et al. Activation energy paths for graphene nucleation and growth on Cu. *ACS Nano* 2012;6(4):3614–23.
- [9] Celebi K, Cole MT, Choi JW, Wyczisk F, Legagneux P, Rupesinghe N, et al. Evolutionary kinetics of graphene formation on copper. *Nano Lett* 2013;13(3):967–74.
- [10] Tsen AW, Brown L, Levendorf MP, Ghahari F, Huang PY, Havener RW, et al. Tailoring electrical transport across grain boundaries in polycrystalline graphene. *Science* 2012;336(6085):1143–6.
- [11] Wahl EH, Owano TG, Kruger CH, Zalicki P, Ma Y, Zare RN. Measurement of absolute CH₃ concentration in a hot-filament reactor using cavity ring-down spectroscopy. *Diamond Relat Mater* 1996;5(3–5):373–7.
- [12] Bhaviripudi S, Jia XT, Dresselhaus MS, Kong J. Role of kinetic factors in chemical vapor deposition synthesis of uniform large area graphene using copper catalyst. *Nano Lett* 2010;10(10):4128–33.
- [13] Watwe RM, Bengaard HS, Rostrup-Nielsen JR, Dumesic JA, Norskov JK. Theoretical studies of stability and reactivity of CH_x species on Ni(111). *J Catal* 2000;189(1):16–30.
- [14] Zhang WH, Wu P, Li ZY, Yang JL. First-principles thermodynamics of graphene growth on Cu surfaces. *J Phys Chem C* 2011;115(36):17782–7.
- [15] Saito R, Hofmann M, Dresselhaus G, Jorio A, Dresselhaus MS. Raman spectroscopy of graphene and carbon nanotubes. *Adv Phys* 2011;60(3):413–550.
- [16] Yu Q, Jauregui LA, Wu W, Colby R, Tian J, Su Z, et al. Control and characterization of individual grains and grain boundaries in graphene grown by chemical vapour deposition. *Nat Mater* 2011;10(6):443–9.
- [17] Ryu S, Liu L, Berciaud S, Yu Y-J, Liu H, Kim P, et al. Atmospheric oxygen binding and hole doping in deformed graphene on a SiO₂ substrate. *Nano Lett* 2010;10(12):4944–51.
- [18] Hofmann M, Shin YC, Hsieh YP, Dresselhaus MS, Kong J. A facile tool for the characterization of two-dimensional materials grown by chemical vapor deposition. *Nano Res* 2012;5(7):504–11.
- [19] Van Den Brekel CHJ, Bollen LJM. Low pressure deposition of polycrystalline silicon from silane. *J Cryst Growth* 1981;54(2):310–22.
- [20] Dutt MB, Sen SK, Barua AK. The diffusion of nickel into copper and copper–nickel alloys. *Physica Status Solidi* 1979;56(1):149–55.
- [21] Norskov JK, Bligaard T, Hvolbaek B, Abild-Pedersen F, Chorkendorff I, Christensen CH. The nature of the active site in heterogeneous metal catalysis. *Chem Soc Rev* 2008;37(10):2163–71.
- [22] Zhou DH, Ma D, Wang Y, Liu XC, Bao XH. Study with density functional theory method C–H bond activation on the MoO₂/HZSM-5 on methane active center. *Chem Phys Lett* 2003;373(1–2):46–51.
- [23] Kim MH, Lee EK, Jun JH, Kong SJ, Han GY, Lee BK, et al. Hydrogen production by catalytic decomposition of methane over activated carbons: kinetic study. *Int J Hydrogen Energy* 2004;29(2):187–93.
- [24] Becker A, Hutterer KJ. Chemistry and kinetics of chemical vapor deposition of pyrocarbon – IV – pyrocarbon deposition from methane in the low temperature regime. *Carbon* 1998;36(3):213–24.
- [25] An W, Zeng XC, Turner CH. First-principles study of methane dehydrogenation on a bimetallic Cu/Ni(111) surface. *J Chem Phys* 2009;131(17):174702.
- [26] Wu P, Zhang W, Li Z, Yang J, Hou JG. Communication: coalescence of carbon atoms on Cu (111) surface. Emergence of a stable bridging-metal structure motif. *J Chem Phys* 2010;133(7):071101.
- [27] Gaddam S, Bjelkevig C, Ge S, Fukutani K, Dowben PA, Kelber JA. Direct graphene growth on MgO: origin of the band gap. *J Phys Condens Matter* 2011;23(7):072204.
- [28] Medina H, Lin YC, Jin CH, Lu CC, Yeh CH, Huang KP, et al. Metal-free growth of nanographene on silicon oxides for transparent conducting applications. *Adv Funct Mater* 2012;22(10):2123–8.
- [29] Al-Temimy A, Riedl C, Starke U. Low temperature growth of epitaxial graphene on SiC induced by carbon evaporation. *Appl Phys Lett* 2009;95(23).